HHS Public Access

Author manuscript

Oncogene. Author manuscript; available in PMC 2011 February 11.

Published in final edited form as:

Oncogene. 2010 August 5; 29(31): 4460–4472. doi:10.1038/onc.2010.199.

A Mosaic Mouse Model of Astrocytoma Identifies αvβ8 Integrin as an Essential Regulator of Tumor-Induced Angiogenesis

Jeremy H. Tchaicha[†], **Aaron K. Mobley**[†], **Mohammad G. Hossain**[†], **Kenneth D. Aldape**[¥], and **Joseph H. McCarty**[†,*]

[†]Department of Cancer Biology, University of Texas M.D. Anderson Cancer Center, 1515 Holcombe Boulevard, Houston, Texas, USA, 77030

[¥]Department of Pathology, University of Texas M.D. Anderson Cancer Center, 1515 Holcombe Boulevard, Houston, Texas, USA, 77030

Abstract

The process of angiogenesis involves a complex set of cell-cell and cell-extracellular matrix (ECM) interactions that coordinately regulate new blood vessel growth and maturation. Although many factors that promote angiogenesis have been characterized, the identities and mechanisms of action of many endogenous inhibitors of angiogenesis remain unclear. Furthermore, little is known about how tumor cells selectively circumvent the actions of these inhibitors to drive pathological angiogenesis, a requisite event for tumor progression. Using mosaic mouse models of the malignant brain cancer, astrocytoma, we report that tumor cells induce pathological angiogenesis by suppressing expression of the ECM protein receptor αvβ8 integrin. Diminished integrin expression in astrocytomas cells leads to reduced activation of latent TGFβs, resulting in impaired TGFβ receptor signaling events in tumor-associated endothelial cells. These data reveal that astrocytoma cells manipulate their angiogenic balance by selectively suppressing αvβ8 integrin expression/function, and also demonstrate that an adhesion and signaling axis normally involved in developmental brain angiogenesis is pathologically exploited in adult brain tumors.

Keywords

glioma; glioblastoma multiforme; extracellular matrix; itgb8; TGFβ; astrocyte

Introduction

The mammalian brain is a highly vascularized organ, with neural cells and blood vessels communicating via direct cell-cell contacts as well as secreted growth factors and ECM proteins (Bautch and James, 2009; McCarty, 2009a). Integrins are cell surface receptors for many ECM ligands (Desgrosellier and Cheresh, 2010), and integrin-mediated adhesion and

*Corresponding author: Department of Cancer Biology, Unit 173 University of Texas, M.D. Anderson Cancer Center 1515 Holcombe Boulevard Houston, TX 77030 jhmccarty@mdanderson.org.

Conflict of Interest Statement: The authors declare no conflict of interest.

signaling events play vital roles in vascular development and homeostasis in the brain (McCarty, 2009b). In particular, the neuroepithelial cell-expressed integrin, αvβ8, is essential for normal blood vessel growth and maturation during brain development (McCarty *et al*., 2002; Zhu *et al*., 2002). Selective ablation of αv or β8 integrin gene expression in embryonic mouse neural progenitors and astrocytes causes brain-specific vascular phenotypes, including endothelial cell hyperplasia, the formation of blood vessels with glomeruloid-like tufts, and intracerebral hemorrhage (McCarty *et al*., 2004; Proctor *et al*., 2005). αvβ8 integrin is a receptor for latent forms of TGFβ1 and TGFβ3 and mediates their bioactivation (Cambier *et al*., 2005). Perturbation of integrin-mediated activation of latent TGFβ1 and TGFβ3, leads to brain-specific vascular defects that phenocopy the pathologies in integrin knockouts (Mu *et al*., 2008). Hence, αvβ8 integrin-mediated TGFβ activation and signaling controls normal cerebral blood vessel morphogenesis and blood-brain barrier development.

In the post-natal brain αvβ8 integrin is expressed in neural stem and progenitor cells (Mobley *et al*., 2009), which are likely cells of origin for the malignant brain cancer astrocytoma (Alcantara Llaguno *et al*., 2009; Zheng *et al*., 2008). High-grade astrocytomas, or glioblastoma multiforme (GBM), are defined in part by the development of hallmark angiogenesis pathologies, including vascular cell hyperproliferation and hemorrhage owing to breakdown of the intratumoral blood-brain barrier (Jain *et al*., 2007; Kaur *et al*., 2004). As detailed above, these tumor-induced vascular pathologies are strikingly similar to phenotypes that develop in mice that are genetically deficient for αvβ8 integrin-mediated activation of TGFβ1 and TGFβ3. Whether astrocytoma cells manipulate integrin-mediated TGFβ activation and signaling pathways to induce pathological angiogenesis, however, remains uncertain. Here, we report that diminished αvβ8 integrin expression and function in astrocytoma cells plays a central role in promoting pathological angiogenesis and abnormal vascular permeability. These results are the first to link deregulation of αvβ8 integrin function to vascular pathologies that are defining features of high-grade astrocytomas.

Results

Analysis of αvβ8 integrin protein expression in human astrocytoma cell lines

Based on the brain-specific angiogenesis phenotypes that develop in αv and β8 integrin knockout mice, we hypothesized that abnormal αvβ8 integrin expression or function may also contribute to angiogenesis pathologies in malignant brain tumors. Therefore, lysates from five established human astrocytoma cell lines were immunoblotted to determine expression levels of αv and β8 integrin proteins. As shown in Figure 1A, differing levels of β8 integrin protein expression were detected in the various human cell lines. U87 and LN18 cells expressed low levels of β8 integrin, whereas LN229, U251, and SNB19 astrocytoma cells expressed robust levels of β8 integrin protein. αv integrin protein levels were constant in the different astrocytoma cell lines, likely owing to the reported expression of other integrin β subunits, e. g., β3 and β5, that heterodimerize with αv integrin (Skuli *et al*., 2009). In order to establish in vivo links between β8 integrin protein levels and tumor-induced angiogenesis, U87 cells or SNB19 cells were stereotactically injected into the brains of immunocompromised mice. All mice injected with U87 cells (n=5, 5×10^5 cells per mouse)

developed neurological deficits within six weeks post-injection. Macroscopic analyses of perfused brains revealed large, well-vascularized and hemorrhagic primary tumors that filled most of the injected hemisphere (Supplemental Figure 1A). Immunohistochemical analyses of sections from U87 tumors using an antibody directed against the endothelial cell-expressed protein CD34 revealed intratumoral blood vessels with distended and sinusoidal-like morphologies (Figure 1C). Mice implanted with SNB19 cells (n=3, 5×10^5 cells injected per mouse) also developed neurological phenotypes within six weeks after implantation; however, intracranial SNB19 tumors were not macroscopically apparent (Supplemental Figure 1B). Microscopic analysis of H&E-stained brain sections from SNB19 tumor-bearing mice revealed focal lesions, often in periventricular regions of the brain (Figure 1D). Anti-CD34 immunohistochemistry (Figures 1E) revealed that microvessels within SNB19 tumors were relatively uniform in diameter, non-hemorrhagic, and morphologically distinct from vessels in U87 tumors (Figure 1C).

Isolation of Primary Astroglial Progenitor Cells from Wild Type and β8−/− Neonatal Mice

Although the analyses of the human astrocytoma cell lines and resulting xenograft tumors suggest intriguing connections between β8 integrin expression and intratumoral vascular pathologies (Figure 1), there are many limitations associated with studying glioma cell lines. For example, these various cell lines have been sequentially passaged over several years, harbor different genetic alterations, and do not express markers commonly expressed in astrocytomas in situ (Ishii *et al*., 1999). Therefore, we decided to analyze functions for β8 integrin in tumor-induced angiogenesis using a more genetically tractable model of astrocytoma.

Astroglial cells, which are putative cells of origin for astrocytomas, were cultured from cerebral cortices of post-natal wild type (+/+) or β8 integrin homozygous (β8−/−) mutant mice. Newborn β8−/− mice were easily distinguished from control littermates by macroscopically apparent intracerebral hemorrhage (Figure 2A and 2C); however, all genotypes were confirmed by PCR-based methods using genomic DNA isolated from tail snips as previously described (Zhu *et al*., 2002). As shown in Figures 2B and 2D, nearly all wild type and β8−/− primary cells were immunoreactive for Nestin, a marker for neural progenitor cells in the brain (Stipursky and Gomes, 2007). Most cells also expressed glial fibrillary acidic protein (GFAP), a marker for differentiated astrocytes and some neural stem cells within the post-natal brain (Mori *et al*., 2005). Based on co-expression of Nestin and GFAP in the majority of cells, we will refer to these cells throughout this report as ‘astroglial progenitors’. In order to determine αvβ8 integrin protein expression in primary astroglial progenitors, cells were surface-labeled with an amine-reactive derivative of biotin. Anti-integrin antibodies were then used to immunoprecipitate integrin proteins from detergent-soluble lysates. Primary wild type astroglial progenitors expressed αvβ5 and αvβ8 integrins (Figure 2E), which is consistent with previous reports for αv integrin expression in primary human astrocytes (Cambier *et al*., 2005). β8−/− astroglial progenitors expressed αvβ5 integrin protein at levels similar to wild type cells, but did not express the αvβ8 integrin heterodimer, owing to β8 integrin gene ablation (Figure 2E). αvβ1, αvβ3 and αvβ6 integrins were not detected in primary astroglial progenitor cells isolated from wild type and

knockout mice (data not shown). Lastly, primary wild type and β8−/− cells did not display obvious differences in proliferation under adherent growth conditions (Figure 2F).

Oncogene-Mediated Transformation of Primary Astroglial Progenitor Cells Leads to Diminished αvβ8 Integrin Expression

Astroglial progenitors were immortalized and transformed using retroviral-delivered oncogenes that target growth pathways commonly altered during astrocytoma initiation and progression. Cells were first immortalized with a retrovirus expressing the human papilloma virus E6 and E7 proteins (Sonoda *et al*., 2001b), which inhibit the expression and function of the p53 and Rb tumor suppressors, respectively. The p53 gene is commonly mutated or deleted in human gliomas (Furnari *et al*., 2007); furthermore, both Rb and p53 negatively regulate the functions of the Ink4a/Arf tumor suppressors, which are commonly deleted in malignant astrocytomas (Bachoo *et al*., 2002; Uhrbom *et al*., 2002). Pooled populations of immortalized cells were then transformed using a retrovirus expressing oncogenic H-Ras (^{G12V}H-Ras) (Sonoda *et al*., 2001b). Ras activities are often hyperactivated in astrocytomas, owing to gene mutations or elevated expression of upstream receptor tyrosine kinases (Holland *et al*., 2000). Two independent preparations of wild type and β8−/− transformed cells were generated using primary cells isolated from different neonatal mice. All in vitro and in vivo results presented below represent one of the two preparations; however, parallel experiments with the second preparation of transformed cells generated similar outcomes (data not shown).

Oncogene-transformed astroglial progenitors maintained Nestin protein expression (Figures 3A, B). Immunoblot analyses confirmed similar levels of Ras and E7 protein overexpression in transformed cells (Figure 3C). We detected increased expression of CD133/Prominin-1, a transmembrane protein that marks some embryonic neural stem cells (Uchida *et al*., 2000) and tumor-initiating cells in GBM and other solid malignancies (Bao *et al*., 2006a; O'Brien *et al*., 2007; Singh *et al*., 2004) following cell transformation (Figure 3D). There was a complete loss of expression of GFAP following cell transformation; in contrast, Nestin protein levels remained unchanged (Figure 3D). This upregulation of CD133/Prominin-1 and down-regulation of GFAP expression suggests oncogene-induced cell "dedifferentiation", similar to what others have proposed for transformed astroglia (Bachoo *et al*., 2002; Uhrbom *et al*., 2002). Lastly, genetic ablation of β8 integrin did not alter adherent growth properties of transformed astroglial progenitor cells (Figure 3E), and wild type and β8−/− transformed cells also generated similar numbers of colonies in three-dimensional soft agar growth assays (Figure 3F).

Transformed wild type cells showed significantly reduced levels of αv and β8 integrin proteins, although the levels of β1 integrin protein were not altered in wild type or β8−/− transformed cells (Figure 4A). Due to a dearth of β8 integrin antibodies available for fluorescent activated cell sorting, integrin expression was quantified in primary versus transformed cells using an anti-αv antibody. As shown in Figure 4B, approximately 90% of wild type and β8−/− primary cells expressed detectable levels of cell surface αv integrin protein. In contrast, oncogene-mediated transformation resulted in an approximately 50% reduction in αv integrin protein expression (Figure 4B). Since β8 integrin heterodimerizes

exclusively with the αv subunit (Milner *et al*., 2001), the reduction in β8 protein levels in wild type transformed cells is likely due to reduced levels of αv integrin protein; indeed, αv protein levels are reduced in oncogene-transformed β8−/− cells (Figure 4B). We have also detected reduced levels of β5 integrin, which also heterodimerizes exclusively with αv integrin, in wild type and β8−/− transformed astroglial cells (data not shown). Levels of αvβ8 integrin protein expression progressively diminished following sequential passaging of wild type transformed astroglial cells (Figure 4C). The diminished αvβ8 integrin protein expression in highly passaged transformed cells was not a secondary consequence of long-term growth in vitro, since we did not detect diminished integrin expression in sequentially passaged primary mouse neurospheres isolated from the post-natal subventricular zone (Supplemental Figure 2).

Analysis of β8 Integrin-Dependent Angiogenesis and Vascular Permeability

The ability of transformed astroglial progenitors to form astrocytoma-like tumors in vivo was analyzed by stereotactically implanting wild type and β8−/− cells into the striatum of immunocompromised mice. Due to the progressive loss of αvβ8 integrin expression in high-passage cells (Figure 4C), all studies were performed with cells cultured for less than four passages following oncogene transformation. All mice injected with either wild type or β8−/− transformed astroglial progenitors developed neurological phenotypes and died within 45 days after injection. Microscopic examination of brains injected with wild type and β8−/− transformed cells (n=20 mice per genotype) revealed tumor formation in 100% of experimental animals.

In comparison to wild type tumors, there were striking differences in the macroscopic appearance of tumors generated from transformed β8−/− astroglial progenitors (Figure 5A, B). Most β8−/− tumors (17 of 20 analyzed) displayed grossly obvious intratumoral hemorrhage; in contrast, only two of 20 wild type astrocytomas showed grossly obvious hemorrhage. Similar results were observed following the injection of transformed αv−/− astroglial cells (data not shown). Kaplan-Meier survival plots revealed that mice with β8−/− tumors (n=16) died significantly earlier than mice harboring wild type tumors (n=20). As shown in Figure 5C, 50% of mice with β8−/− tumors were alive at 26 days post-implantation, whereas mice harboring wild type tumors showed 50% survival at 33 days. The most probable reason for the accelerated death of mice bearing β8−/− astrocytomas relates to the severe intratumoral hemorrhage in these animals. We have noticed that extravasated red blood cells accumulate in the brain ventricles and likely obstruct the flow of cerebrospinal fluid, leading to hydrocephalus and neurological deficits. In a separate cohort of mice, we compared tumor volumes at 14 and 21 days after intracranial injection of wild type and β8−/− transformed cells (n=9 mice per genotype per time point). Tumor volumes were quantified in H&E-stained brain sections by measuring tumor diameter at the largest cross-sectional area; however, no obvious differences were detected in sizes of tumors derived from wild type and β8−/− transformed cells at 14 and 21 days post-implantation (Figure 5D).

Microscopic analysis of H&E-stained tumor sections revealed that wild type tumors (Figure 6A) were highly vascularized and displayed pathological features similar to grade III

anaplastic astrocytoma, consistent with previous reports (Sonoda *et al*., 2003; Sonoda *et al*., 2001a). H&E-stained sections from β8−/− tumors, however, revealed hemorrhagic blood vessels with tortuous and distended morphologies (Figure 6B). Both wild type and β8−/− intratumoral blood vessels were lined with CD34-expressing vascular endothelial cells (Figure 6C, D); however, immunofluorescence-based quantitation revealed significantly more CD34-expressing vessels within β8−/− tumors (Figure 6G). The severe vascular pathologies within β8−/− tumors made them more similar to grade IV GBM, although other defining features of human GBM, such as regions of pseudopallisading necrosis were not evident in β8−/− tumors (data not shown).

Pericytes are vascular mural cells that closely juxtapose endothelial cells and are necessary for normal blood vessel structure and function (Adams and Alitalo, 2007). Therefore, we analyzed whether microvascular pericytes were present in wild type and β8−/− astrocytomas. Most CD34-expressing endothelial cells in wild type astrocytomas were associated with Desmin^{+} pericytes (Figure 6E). β8−/− tumors displayed increased numbers of CD34-expressing blood vessels with distended and tortuous morphologies; however, vessels within β8−/− tumors were also associated with Desmin-expressing pericytes (Figure 6F).

Wild type or β8−/− tumor cells did not express detectable levels of GFAP in vivo, although non-malignant reactive astrocytes that formed a glial scar around the tumor margins displayed robust GFAP expression (Supplemental Figure 3C). Wild type and β8−/− cells maintained Nestin expression and displayed similar patterns of perivascular invasiveness (Supplemental Figure 3A, B).

Rescue of Vascular Pathologies by Forced Expression of β8 Integrin Protein in β8−/− Cells

In order to determine whether the vascular pathologies in β8−/− tumors were the direct result of loss of β8 integrin protein, or were due to integrin-independent effects on cell transformation, we restored β8 integrin protein expression in β8−/− cells using a plasmid expressing human β8 integrin protein tagged at the C-terminus with the V5 epitope. Protein expression was confirmed by immunoblotting with anti-β8 or anti-V5 antibodies (Figure 7A).

β8−/− cells stably transfected with empty pcDNA4 plasmid were stereotactically injected into the striatum of immunocompromised mice (n=5). Resulting intracranial tumors were hemorrhagic and contained dilated blood vessels (Figures 7B, D, F). In contrast, injection of β8−/− cells forcibly expressing β8V5 integrin protein (n=5 mice) generated tumors with blood vessels that were fairly uniform in size and non-hemorrhagic (Figures 7B, C, E). These data demonstrate that the severe vascular pathologies in β8−/− tumors are caused by loss of β8 integrin expression and function, and that these vascular defects can be largely reversed following exogenous expression of β8 integrin protein.

Analysis of Integrin-Dependent VEGF Expression

Prior reports demonstrated that VEGF plays important roles in pathological angiogenesis and hemorrhage within brain tumors (Benjamin and Keshet, 1997; Cheng *et al*., 1996;

Cheng *et al*., 1997; Kanamori *et al*., 2004). Since these pathologies are similar to what we have observed in β8−/− astrocytomas (Figures 5 and 6), levels of VEGF mRNA and protein expression were analyzed in transformed astroglial progenitors and tumors. As shown in Supplemental Figure 4A, we detected decreased expression of the VEGF120 and VEGF164 mRNAs in β8−/−cells. Analysis of VEGF protein expression by ELISA also revealed approximately 50% less VEGF in conditioned media from β8−/− cells (Supplemental Figure 4B), further indicating that β8 integrin positively regulates VEGF gene expression. VEGF expression was also analyzed by immunoblotting detergent-soluble lysates prepared from wild type and β8−/− astrocytomas (n=2 tumors per genotype). However, we did not detect differences in VEGF protein expression (Supplemental Figure 4C), likely owing to VEGF expression by non-malignant stromal cells. Along these lines, immunofluorescence staining of wild type and β8−/− tumors with an anti-VEGF antibody revealed no obvious differences in VEGF protein expression (Supplemental Figure 4D, E).

Analysis of Integrin-Dependent TGFβ Activation and Signaling

We next analyzed integrin-dependent TGFβ expression, activation and receptor signaling in transformed astroglial cells and astrocytomas. Integrin-dependent differences in expression of TGFβ1, TGFβ2 and TGFβ3 mRNAs in transformed cells were not obvious as assessed by semi-quantitative RT-PCR (data not shown). β8 integrin-mediated activation of latent TGFβ1 was measured in vitro using luciferase reporter assays. Wild type or β8−/− transformed astrocytes were exposed to 10 ng/ml latent TGFβ1 for 12 hours, and conditioned media was then added to mink lung epithelial cells stably transfected with a reporter plasmid containing a truncated plasminogen activator inhibitor-1 (PAI-1) promoter driving expression of firefly luciferase (PAI1-luciferase) (Abe *et al*., 1994). As shown in Figure 8A (black bars), in comparison to conditioned media from wild type cells, there was a significant reduction (approximately 30%) in luciferase activity using conditioned media from β8−/− cells. These data reveal that αvβ8 integrin in astrocytoma cells promotes, in part, the activation of latent TGFβ1. However, in the absence of LAP-TGFβ1 a statistically significant increase in luciferase activity was detected using conditioned media from wild type and β8−/− transformed cells (grey bars in Figure 8A), suggesting integrin-independent mechanisms of latent TGFβ activation.

We reasoned that the three-dimensional context of the brain tumor microenvironment might reveal more dramatic differences in integrin-dependent TGFβ activation/signaling in vascular endothelial cells. Therefore, we analyzed TGFβ signaling events in situ using an antibody directed against phosphorylated Smad3 (pSmad3) protein, a canonical TGFβ signaling protein that translocates into the nucleus following TGFβ receptor-mediated phosphorylation (Massague, 2008). As shown in Figure 8B, $CD31^+$ blood vessels within β8 integrin-expressing astrocytomas displayed robust levels of nuclear pSmad3 protein. In contrast, most $CD31^+$ blood vessels within β8−/− tumors expressed low or undetectable levels of nuclear pSmad3 (Figure 8C). In order to more quantitatively assess integrin-mediated TGFβ signaling, vascular endothelial cells were sorted from tumors using magnetic beads coated with anti-CD31 antibodies. Freshly prepared cell lysates were then immunoblotted with antibodies directed against phosphorylated forms of Smad2 and Smad3. As shown in Figure 8D, a reduction in phosphorylation of Smad2/3 was apparent in CD31-

expressing cells sorted from β8−/− tumors. Laser scanning densitometry was used to quantify the band intensities, revealing that vascular endothelial cells isolated from β8−/− tumors expressed two-fold less total Smad2/3 protein levels. These data suggest that αvβ8 integrin regulates Smad2/3 protein stability in endothelial cells. The phospho-Smad2/3 band intensities were then normalized to the total Smad2/3 levels; however, we still detected two-fold less pSmad2 and three-fold less pSmad3 in CD31 lysates from β8−/− tumors. These data reveal that the vascular pathologies in astrocytomas correlate with impaired integrin-mediated TGFβ activation and signaling via Smad2 and Smad3 in intratumoral endothelial cells.

Discussion

A major conclusion from this study is that αvβ8 integrin, an ECM protein receptor that we have previously shown to be essential for embryonic brain angiogenesis, also plays a key role in regulating pathological angiogenesis astrocytomas growing in the adult brain. Our data reveal the following specific findings: (i) αvβ8 integrin is differentially expressed in human astrocytoma cell lines, with low levels of integrin expression correlating with increased intratumoral angiogenesis and hemorrhage (Figure 1); (ii) primary mouse astroglial progenitor cells, which are presumptive cells of origin for astrocytomas, express robust levels of αvβ8 integrin protein (Figure 2); (iii) oncogene-mediated transformation of astroglial progenitors results in a progressive reduction in αvβ8 integrin protein expression (Figures 3 and 4); (iv) stereotactic injection of transformed wild type astroglial progenitors generates grade III anaplastic astrocytomas, whereas β8−/− cells give rise to tumors with vascular pathologies similar to grade IV GBM (Figures 5 and 6); (v) the severe vascular pathologies in β8−/− tumors are largely ameliorated by exogenous expression of β8 integrin protein (Figure 7); and (vi) β8−/− astrocytoma cells are partially impaired in their ability to activate latent TGFβs and stimulate TGFβ signaling pathways in tumor-associated vascular endothelial cells (Figure 8).

αvβ8 integrin-dependent interplay between TGFb and VEGF signaling pathways

αvβ8 integrin is expressed in astrocytes and neural stem cells in the adult mouse brain, where it negatively regulates blood vessel growth and permeability (Mobley *et al*., 2009). However, various reports have also shown that stem-like GBM cells, which are likely derived from neural stem cells and/or astrocytes, induce robust pathological angiogenesis to initiate and sustain tumor growth and progression (Bao *et al*., 2006b; Calabrese *et al*., 2007). We propose that one mechanism used by newly stem-like tumor cells to circumvent the negative regulatory effects of αvβ8 integrin and drive progression to more malignant stages is via down-regulating integrin expression and function. Diminished integrin expression, combined with expression of pro-angiogenesis factors, e.g., VEGF, likely promotes neovessel formation necessary for tumor growth and progression. VEGF overexpression alone, however, is not sufficient to generate vascular pathologies in GBM, suggesting the need for dysregulation of other pathways (Sonoda *et al*., 2003). Interestingly, TGFβs has been reported to inhibit the pro-angiogenic and pro-permeability actions of VEGF (Ramsauer and D'Amore, 2007). Here, we report a correlation between decreased integrin-mediated activation of latent TGFβs and TGFβ signaling and enhanced angiogenesis and

vascular permeability, (Figures 5-8), supporting a model whereby integrin-activated TGFβs counteract the effects of VEGF (Supplemental Figure 5). TGFβ-mediated Smad3 phosphorylation in tumor cells has also been reported to enhance VEGF gene expression (Petersen *et al*.). Interestingly, β8−/− astrocytoma cells, which have diminished TGFβ activation capacities (Figure 8), express reduced levels VEGF mRNA and protein (Supplemental Figure 4). Collectively, these data suggest that integrin-mediated TGFβ activation negatively regulates VEGF gene expression and VEGF receptor signaling pathways during astrocytoma angiogenesis.

A potential role for αvβ8 integrin as a suppressor of astrocytoma progression

The dramatic reduction in αvβ8 integrin protein expression that occurs following oncogene-mediated cell transformation also suggests that this integrin may play a suppressive role in tumor growth and/or progression. Although complete genetic ablation of β8 integrin expression does not lead to spontaneous brain tumorigenesis (Mobley *et al*., 2009), it is possible that other genetic alterations, e. g., activation of oncogenes or loss of a tumor suppressor functions may act in concert with diminished β8 integrin expression to promote spontaneous tumorigenesis. We have shown that genetic ablation of αv integrin in epithelial cells of the skin leads to the progressive development of squamous cell carcinoma over several post-natal months (McCarty *et al*., 2008), suggesting that genetic alterations acting in combination with loss of integrin expression contribute to tumorigenesis. Interestingly, in transformed astroglial cells β8 integrin protein expression is diminished at high passage numbers (Figure 4C), which correlates with a timeline when astrocytes undergo spontaneous loss of the p53 locus (Bogler *et al*., 1995). We are currently investigating functional links between αvβ8 integrin with oncogene and suppressor pathways in astrocytomas.

αvβ8 integrin and human gliomagenesis

In the only other published report for β8 integrin in brain tumorigenesis, Louis and colleagues showed increased expression of β8 integrin mRNA in human GBM samples (Riemenschneider *et al*., 2005). These analyses centered on integrin expression in primary GBMs, which arise de novo and harbor some genetic alterations that are distinct from secondary GBMs, which are more similar to the mosaic models that we have analyzed in this study. Hence, there may be distinct functions for αvβ8 integrin in primary versus secondary GBMs, possibly related to different genetic lesions contributing to tumor initiation and progression. Additionally, the non-malignant samples analyzed by Louis and colleagues were from cerebral cortices, and not from the subventricular zone, which harbors neural stem and progenitor cells that likely give rise to GBMs (Alcantara Llaguno *et al*., 2009; Zheng *et al*., 2008). It is also possible that sub-populations of GBM cells, e.g., those with stem-like properties that cluster around blood vessels (Bao *et al*., 2006b; Calabrese *et al*., 2007), have diminished αvβ8 integrin expression/function. Any differences in integrin expression in this minority population of cells, however, would not be detected by analyzing bulk tumor masses. We are currently investigating the expression of αvβ8 integrin in low- and high-grade human astrocytomas to further determine the functions of this integrin in tumor-induced angiogenesis and other malignant processes.

Materials and Methods

Mice and Genotyping

Male NCR$^{nu/nu}$ mice were purchased from Jackson Laboratories and used for all experiments involving intracranial injections of mouse and human astrocytoma cells. β8+/− mice were obtained from the Mutant Mouse Regional Resource Center.

Antibodies, Immunoblotting and Immunofluorescence

The affinity-purified anti-αv polyclonal antibody was generated by our laboratory using a synthetic peptide (CKRVRPPQEEQEREQLQPHENGEGTSEA) corresponding to a region of the chicken αv cytoplasmic domain. The anti-β8 integrin antibody used for all immunoblotting has been described previously (McCarty *et al*., 2005; McCarty *et al*., 2004). The following antibodies were purchased: rabbit anti-β1 integrin, rabbit anti -β5 integrin, rabbit anti-nestin, and rat anti-mouse CD133 (Chemicon), rat anti-mouse CD34 mAb (Genetex), chicken anti-Nestin IgY (Neuromics), rat anti-mouse CD31 and rat anti-mouse αv-PE mAbs (BD Biosciences), rabbit anti-β-actin pAb (Sigma), rabbit anti-GFAP pAb (DAKO), rabbit anti-pSmad3 mAb (Epitomics), and anti-Ras and anti-E7 antibodies (Santa Cruz Biotech). Mouse anti-VEGF, rabbit anti-Desmin, as well as rabbit anti-pSmad2 and tSmad2/3 antibodies were purchased from Cell Signaling Technologies. The anti-V5 mAb was purchased form Clontech Laboratories. Secondary antibodies were goat anti-rabbit, goat anti-chicken, goat anti-rat and goat anti-mouse, all conjugated to Alexa488 or Alexa594 (Molecular Probes). For quantitation of blood vessel densities, digital images were captured from sections stained for CD34 immunofluorescence. Mean fluorescence intensity was calculated using ImageJ software. Two investigators, who were blinded to the genotypes for each sample, analyzed fluorescent sections.

Isolation and Propagation of Murine Astroglial Progenitors and Human Astrocytoma Cell Lines

Astroglial progenitors were cultured from cerebral cortices of wild type or β8−/− neonates (P0-P3) and propagated on laminin-coated dishes, as described previously (McCarty *et al*., 2005). To generate retroviral stocks, 293T Phoenix cells were transfected with pLXSP-puro-E6/E7 and pLXSN-neo-^{G12V}H-Ras (Sonoda *et al*., 2001b). Primary astroglial cells were transduced with the E6/E7 retroviral supernatant and cells were selected in growth media containing 1 μg/ml puromycin for 5 days. Puromycin-resistant clones were pooled and transduced with ^{G12V}H-Ras retrovirus supernatant, and selected after 10 days in G418 (900 μg/ml). To analyze integrin expression in passaged cells, semi-confluent monolayers of cells were trypsinized and split 1:5 onto new dishes. After reaching 80-90% confluence the procedure was repeated. Transformed β8−/− cells were transfected with empty vector (pcDNA4-V5) or vector containing the full-length human β8 integrin cDNA (pcDNA4-β8V5) (McCarty *et al*., 2005; McCarty *et al*., 2004). Stable transfectants were selected by growth in Zeocin (300 μg/ml) for 10 days, and integrin overexpression was confirmed by immunoblotting lysates with anti-β8 or anti-V5 antibodies. U87 and LN229 astrocytoma cells were purchased form American Tissue Culture Collection (ATCC) and were propagated in DMEM/F12 supplemented with 10% bovine serum and antibiotics. U251 and SNB19 cells were kindly provided by Drs. Oliver Bogler and Dimpy Koul (both at

MDACC), respectively, and were grown in DMEM/F12 supplemented with 10% bovine serum and antibiotics.

Soft Agar Growth Assays

A 1% solution of sterile DNA-grade agarose was mixed with 2X DMEM medium, and the 1X base solution was added to 6-well dishes and solidified. The transformed astrocytes (20,000 cells/ml in 2X media) were mixed with a 0.7% agarose solution, and 5,000 cells were added to the base agarose. The plates were incubated at 37° C for one to two weeks. Cells were fixed with 4% PFA/PBS and stained with 0.1% crystal violet.

Intracranial Injections of Transformed Astroglial Cells and Human Astrocytoma Cells

Nude mice were anesthetized and a single incision was made from the anterior pole of the skull to the posterior ridge. A hole was drilled over the target brain structure to expose the brain. We targeted the striatum for cell implantation using the following stereotactic coordinates, all relative to the bregma: 1.5 mm rostral, 1.5 mm anterior, and 4 mm below the pial surface. An automated micropump (Stoelting Instruments) was used to dispense cells in 3 to 5 μl PBS over a five-minute period. Astroglial progenitors cultured for less than four passages after transformation were used for the experiments. In the Kaplan-Meier survival study 2.5×10^4 transformed cells were injected, and animals were monitored until development of tumor-induced neurological phenotypes, ranging from weight loss to ataxia. In other experiments, nude mice were stereotactically injected with 1×10^5 wild type or β8−/− transformed cells and tumor-bearing animals were perfused with 4% PFA/PBS. Brains were coronally sliced at 1 mm intervals and paraffin-embedded tissue was serially sectioned at 7 μm intervals. Human intracranial xenograft tumors were generated by injecting 5×10^5 U87 or SNB19 cells into the striatum of immunocompromised mice.

Isolation of CD31$^+$ Intratumoral Cells

Mice harboring 21 day-old intracranial tumors derived from β8−/− (+ vector) or β8−/− (+ β8V5) transformed astroglial progenitors were sacrificed. Tumors were then microdissected from the brain and dissociated into a single cell suspension using neural tissue dissociation media (Rietze and Reynolds, 2006). CD31-expressing cells were sorted using a rat anti-mouse CD31 antibody (BD Biosciences), magnetic beads coated with goat anti-rat secondary antibody (Miltenyi Biotec, Inc.), and a BioMag magnetic separation unit (Polysciences, Inc.)

Luciferase Reporter Assays

Mink lung epithelial cells stably transfected with a PAI1-Luciferase plasmid (Abe *et al*., 1994) were seeded onto poly-lysine-coated 6-well plates at 4×10^5 cells per well. Twelve hours later media was removed and serum-free media was added for 24 hours. Conditioned media from wild type and β8−/− transformed astroglial progenitor cells pre-incubated for 12 hours with or without 10 ng/ml LAP-TGFβ1 (R&D Systems) was collected and added to MLECs for 12 hours. Cell lysates were then prepared and luciferase substrates were added and quantified using an Enhanced Luciferase Assay Kit (BD Biosciences).

Statistical Analyses

Student's t-test was used to determine statistically significant differences. The Wilcoxan Rank Sum Test was used for analysis of Kaplan-Meier survival results.

Supplementary Material

Refer to Web version on PubMed Central for supplementary material.

Acknowledgments

We are grateful to Drs. Nami McCarty for providing assistance with FACS analysis and Russell Pieper for generously providing E6/E7 and ^{G12V}H-Ras plasmids, respectively. This research was supported by grants awarded to J.H.M. from the National Institutes of Neurological Disease and Stroke (R01NS059876-02), the National Cancer Institute (P50CA127001-02), and the Ellison Medical Foundation (AG-NS-0324-06). This work was also supported in part by a National Cancer Institute core grant (CA-16672) awarded to The University of Texas M. D. Anderson Cancer Center.

References

Abe M, Harpel JG, Metz CN, Nunes I, Loskutoff DJ, Rifkin DB. An assay for transforming growth factor-beta using cells transfected with a plasminogen activator inhibitor-1 promoter-luciferase construct. Anal Biochem. 1994; 216:276–84. [PubMed: 8179182]

Adams RH, Alitalo K. Molecular regulation of angiogenesis and lymphangiogenesis. Nat Rev Mol Cell Biol. 2007; 8:464–78. [PubMed: 17522591]

Alcantara Llaguno S, Chen J, Kwon CH, Jackson EL, Li Y, Burns DK, et al. Malignant astrocytomas originate from neural stem/progenitor cells in a somatic tumor suppressor mouse model. Cancer Cell. 2009; 15:45–56. [PubMed: 19111880]

Bachoo RM, Maher EA, Ligon KL, Sharpless NE, Chan SS, You MJ, et al. Epidermal growth factor receptor and Ink4a/Arf: convergent mechanisms governing terminal differentiation and transformation along the neural stem cell to astrocyte axis. Cancer Cell. 2002; 1:269–77. [PubMed: 12086863]

Bao S, Wu Q, McLendon RE, Hao Y, Shi Q, Hjelmeland AB, et al. Glioma stem cells promote radioresistance by preferential activation of the DNA damage response. Nature. 2006a; 444:756–60. [PubMed: 17051156]

Bao S, Wu Q, Sathornsumetee S, Hao Y, Li Z, Hjelmeland AB, et al. Stem cell-like glioma cells promote tumor angiogenesis through vascular endothelial growth factor. Cancer Res. 2006b; 66:7843–8. [PubMed: 16912155]

Bautch VL, James JM. Neurovascular development: The beginning of a beautiful friendship. Cell Adh Migr. 2009; 3:199–204. [PubMed: 19363295]

Benjamin LE, Keshet E. Conditional switching of vascular endothelial growth factor (VEGF) expression in tumors: induction of endothelial cell shedding and regression of hemangioblastoma-like vessels by VEGF withdrawal. Proc Natl Acad Sci U S A. 1997; 94:8761–6. [PubMed: 9238051]

Bogler O, Huang HJ, Cavenee WK. Loss of wild-type p53 bestows a growth advantage on primary cortical astrocytes and facilitates their in vitro transformation. Cancer Res. 1995; 55:2746–51. [PubMed: 7796398]

Calabrese C, Poppleton H, Kocak M, Hogg TL, Fuller C, Hamner B, et al. A perivascular niche for brain tumor stem cells. Cancer Cell. 2007; 11:69–82. [PubMed: 17222791]

Cambier S, Gline S, Mu D, Collins R, Araya J, Dolganov G, et al. Integrin alpha(v)beta8-mediated activation of transforming growth factor-beta by perivascular astrocytes: an angiogenic control switch. Am J Pathol. 2005; 166:1883–94. [PubMed: 15920172]

Cheng SY, Huang HJ, Nagane M, Ji XD, Wang D, Shih CC, et al. Suppression of glioblastoma angiogenicity and tumorigenicity by inhibition of endogenous expression of vascular endothelial growth factor. Proc Natl Acad Sci U S A. 1996; 93:8502–7. [PubMed: 8710899]

Cheng SY, Nagane M, Huang HS, Cavenee WK. Intracerebral tumor-associated hemorrhage caused by overexpression of the vascular endothelial growth factor isoforms VEGF121 and VEGF165 but not VEGF189. Proc Natl Acad Sci U S A. 1997; 94:12081–7. [PubMed: 9342366]

Desgrosellier JS, Cheresh DA. Integrins in cancer: biological implications and therapeutic opportunities. Nat Rev Cancer. 2010; 10:9–22. [PubMed: 20029421]

Furnari FB, Fenton T, Bachoo RM, Mukasa A, Stommel JM, Stegh A, et al. Malignant astrocytic glioma: genetics, biology, and paths to treatment. Genes Dev. 2007; 21:2683–710. [PubMed: 17974913]

Holland EC, Celestino J, Dai C, Schaefer L, Sawaya RE, Fuller GN. Combined activation of Ras and Akt in neural progenitors induces glioblastoma formation in mice. Nat Genet. 2000; 25:55–7. [PubMed: 10802656]

Ishii N, Maier D, Merlo A, Tada M, Sawamura Y, Diserens AC, et al. Frequent co-alterations of TP53, p16/CDKN2A, p14ARF, PTEN tumor suppressor genes in human glioma cell lines. Brain Pathol. 1999; 9:469–79. [PubMed: 10416987]

Jain RK, di Tomaso E, Duda DG, Loeffler JS, Sorensen AG, Batchelor TT. Angiogenesis in brain tumours. Nat Rev Neurosci. 2007; 8:610–22. [PubMed: 17643088]

Kanamori M, Vanden Berg SR, Bergers G, Berger MS, Pieper RO. Integrin beta3 overexpression suppresses tumor growth in a human model of gliomagenesis: implications for the role of beta3 overexpression in glioblastoma multiforme. Cancer Res. 2004; 64:2751–8. [PubMed: 15087390]

Kaur B, Tan C, Brat DJ, Post DE, Van Meir EG. Genetic and hypoxic regulation of angiogenesis in gliomas. J Neurooncol. 2004; 70:229–43. [PubMed: 15674480]

Massague J. TGFbeta in Cancer. Cell. 2008; 134:215–30. [PubMed: 18662538]

McCarty JH. Cell adhesion and signaling networks in brain neurovascular units. Curr Opin Hematol. 2009a; 16:209–14. [PubMed: 19318941]

McCarty JH. Integrin-mediated regulation of neurovascular development, physiology and disease. Cell Adh Migr. 2009b; 3:211–5. [PubMed: 19372738]

McCarty JH, Barry M, Crowley D, Bronson RT, Lacy-Hulbert A, Hynes RO. Genetic ablation of alphav integrins in epithelial cells of the eyelid skin and conjunctiva leads to squamous cell carcinoma. Am J Pathol. 2008; 172:1740–7. [PubMed: 18467691]

McCarty JH, Cook AA, Hynes RO. An interaction between {alpha}v{beta}8 integrin and Band 4.1B via a highly conserved region of the Band 4.1 C-terminal domain. Proc Natl Acad Sci U S A. 2005; 102:13479–83. [PubMed: 16157875]

McCarty JH, Lacy-Hulbert A, Charest A, Bronson RT, Crowley D, Housman D, et al. Selective ablation of {alpha}v integrins in the central nervous system leads to cerebral hemorrhage, seizures, axonal degeneration and premature death. Development. 2004

McCarty JH, Monahan-Earley RA, Brown LF, Keller M, Gerhardt H, Rubin K, et al. Defective associations between blood vessels and brain parenchyma lead to cerebral hemorrhage in mice lacking alphav integrins. Mol Cell Biol. 2002; 22:7667–77. [PubMed: 12370313]

Milner R, Relvas JB, Fawcett J, ffrench-Constant C. Developmental regulation of alphav integrins produces functional changes in astrocyte behavior. Mol Cell Neurosci. 2001; 18:108–18. [PubMed: 11461157]

Mobley AK, Tchaicha JH, Shin J, Hossain MG, McCarty JH. {beta}8 integrin regulates neurogenesis and neurovascular homeostasis in the adult brain. J Cell Sci. 2009; 122:1842–51. [PubMed: 19461074]

Mori T, Buffo A, Gotz M. The novel roles of glial cells revisited: the contribution of radial glia and astrocytes to neurogenesis. Curr Top Dev Biol. 2005; 69:67–99. [PubMed: 16243597]

Mu Z, Yang Z, Yu D, Zhao Z, Munger JS. TGFbeta1 and TGFbeta3 are partially redundant effectors in brain vascular morphogenesis. Mech Dev. 2008; 125:508–16. [PubMed: 18343643]

O'Brien CA, Pollett A, Gallinger S, Dick JE. A human colon cancer cell capable of initiating tumour growth in immunodeficient mice. Nature. 2007; 445:106–10. [PubMed: 17122772]

Petersen M, Pardali E, van der Horst G, Cheung H, van den Hoogen C, van der Pluijm G, et al. Smad2 and Smad3 have opposing roles in breast cancer bone metastasis by differentially affecting tumor angiogenesis. Oncogene. 29:1351–61. [PubMed: 20010874]

Proctor JM, Zang K, Wang D, Wang R, Reichardt LF. Vascular development of the brain requires beta8 integrin expression in the neuroepithelium. J Neurosci. 2005; 25:9940–8. [PubMed: 16251442]

Ramsauer M, D'Amore PA. Contextual role for angiopoietins and TGFbeta1 in blood vessel stabilization. J Cell Sci. 2007; 120:1810–7. [PubMed: 17502485]

Riemenschneider MJ, Mueller W, Betensky RA, Mohapatra G, Louis DN. In situ analysis of integrin and growth factor receptor signaling pathways in human glioblastomas suggests overlapping relationships with focal adhesion kinase activation. Am J Pathol. 2005; 167:1379–87. [PubMed: 16251422]

Rietze RL, Reynolds BA. Neural stem cell isolation and characterization. Methods Enzymol. 2006; 419:3–23. [PubMed: 17141049]

Singh SK, Hawkins C, Clarke ID, Squire JA, Bayani J, Hide T, et al. Identification of human brain tumour initiating cells. Nature. 2004; 432:396–401. [PubMed: 15549107]

Skuli N, Monferran S, Delmas C, Favre G, Bonnet J, Toulas C, et al. Alphavbeta3/alphavbeta5 integrins-FAK-RhoB: a novel pathway for hypoxia regulation in glioblastoma. Cancer Res. 2009; 69:3308–16. [PubMed: 19351861]

Sonoda Y, Kanamori M, Deen DF, Cheng SY, Berger MS, Pieper RO. Overexpression of vascular endothelial growth factor isoforms drives oxygenation and growth but not progression to glioblastoma multiforme in a human model of gliomagenesis. Cancer Res. 2003; 63:1962–8. [PubMed: 12702589]

Sonoda Y, Ozawa T, Aldape KD, Deen DF, Berger MS, Pieper RO. Akt pathway activation converts anaplastic astrocytoma to glioblastoma multiforme in a human astrocyte model of glioma. Cancer Res. 2001a; 61:6674–8. [PubMed: 11559533]

Sonoda Y, Ozawa T, Hirose Y, Aldape KD, McMahon M, Berger MS, et al. Formation of intracranial tumors by genetically modified human astrocytes defines four pathways critical in the development of human anaplastic astrocytoma. Cancer Res. 2001b; 61:4956–60. [PubMed: 11431323]

Stipursky J, Gomes FC. TGF-beta1/SMAD signaling induces astrocyte fate commitment in vitro: implications for radial glia development. Glia. 2007; 55:1023–33. [PubMed: 17549683]

Uchida N, Buck DW, He D, Reitsma MJ, Masek M, Phan TV, et al. Direct isolation of human central nervous system stem cells. Proc Natl Acad Sci U S A. 2000; 97:14720–5. [PubMed: 11121071]

Uhrbom L, Dai C, Celestino JC, Rosenblum MK, Fuller GN, Holland EC. Ink4a-Arf loss cooperates with KRas activation in astrocytes and neural progenitors to generate glioblastomas of various morphologies depending on activated Akt. Cancer Res. 2002; 62:5551–8. [PubMed: 12359767]

Zheng H, Ying H, Yan H, Kimmelman AC, Hiller DJ, Chen AJ, et al. p53 and Pten control neural and glioma stem/progenitor cell renewal and differentiation. Nature. 2008; 455:1129–33. [PubMed: 18948956]

Zhu J, Motejlek K, Wang D, Zang K, Schmidt A, Reichardt LF. beta8 integrins are required for vascular morphogenesis in mouse embryos. Development. 2002; 129:2891–903. [PubMed: 12050137]

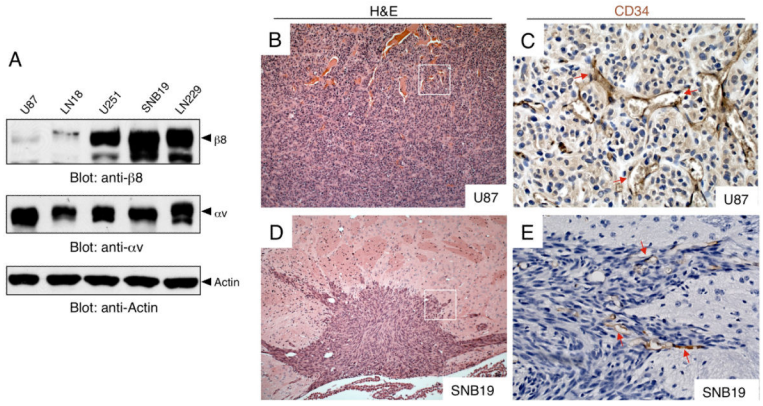

Figure 1. β8 integrin protein is differentially expressed in human astrocytoma cell lines

(A); Detergent-soluble lysates prepared from five human astrocytoma cell lines were immunoblotted with antibodies recognizing αv and β8 integrin proteins. Note that U87 and LN18 cells express low levels of β8 integrin protein, whereas LN229, SNB19 and U251 cell express robust levels of β8 integrin protein. **(B, C);** U87 glioma cells, which express low levels of β8 integrin, were stereotactically implanted into the striatum of immunocompromised mice (n=5) and coronal tumor sections were analyzed by H&E staining (B) or anti-CD34 immunohistochemistry (C). Note that U87 cells form large intracranial tumors that are well vascularized and contain hemorrhagic and sinusoidal-like vessels (arrows in C). Boxed areas in B (100X) are shown at higher magnification (400X) in panel C. **(D, E);** SNB19 glioma cells, which express robust levels of β8 integrin protein, were stereotactically implanted into the striatum of immunocompromised mice (n=3) and coronal tumor sections were analyzed by H&E staining (D) or anti-CD34 immunohistochemistry (E). SNB19 tumors formed in periventricular regions of the brain. These focal lesions contained blood vessels (arrows in E) that are morphologically distinct from blood vessels in U87 tumors (arrows in C). Boxed areas in D (100X) are shown at higher magnification (400X) in panel E.

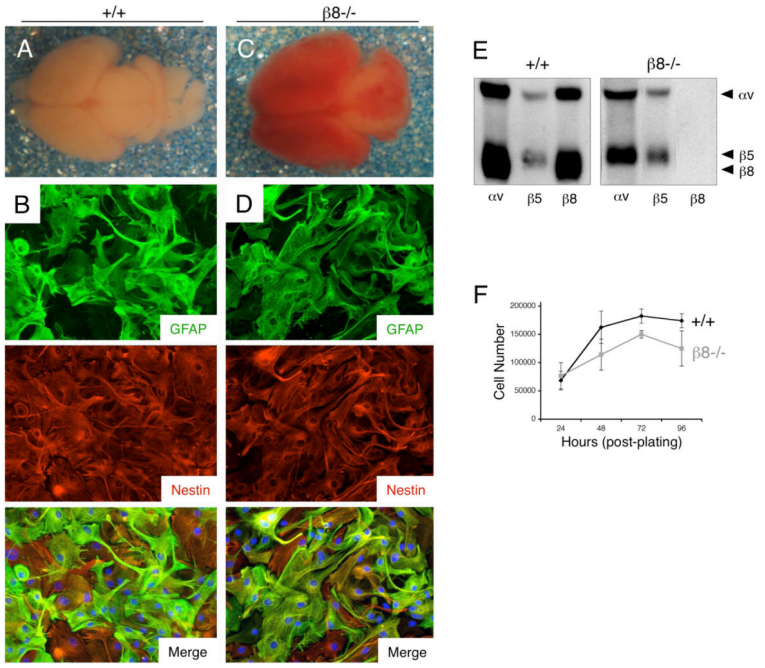

Figure 2. Mouse astroglial progenitor cells, a presumptive cell type of origin for astrocytomas, express robust levels of endogenous αvβ8 integrin

(A, C); Images of whole brains dissected from wild type (A) and β8−/− (C) newborn littermates. Note the hemorrhage throughout the β8 integrin knockout brain. **(B, D);** Primary astroglial progenitor cells were cultured from cerebral cortices of wild type (B) or β8−/− (D) neonatal mice and immunofluorescently stained with antibodies recognizing GFAP (upper panels) and nestin (middle panels). Note that most cells co-express GFAP and Nestin protein (lower panels in B, D). **(E);** Analysis of integrin protein expression in primary astroglial progenitors. Wild type and β8−/− astroglial progenitor cells cultured from neonatal brains were incubated with amine-reactive biotin to label cell surface proteins. Lysates were immunoprecipitated with antibodies directed against αv, β5 or β8 integrins. Note the absence of αvβ8 integrin expression in β8−/− cells. **(F);** Primary β8−/− astroglial progenitor cells do not display obvious growth differences in vitro, as compared to wild type controls. Cell proliferation under adherent conditions was quantified by counting viable cells every 24 hours over a period of four days (n=3 per genotype per time point). Error bars represent standard deviations.

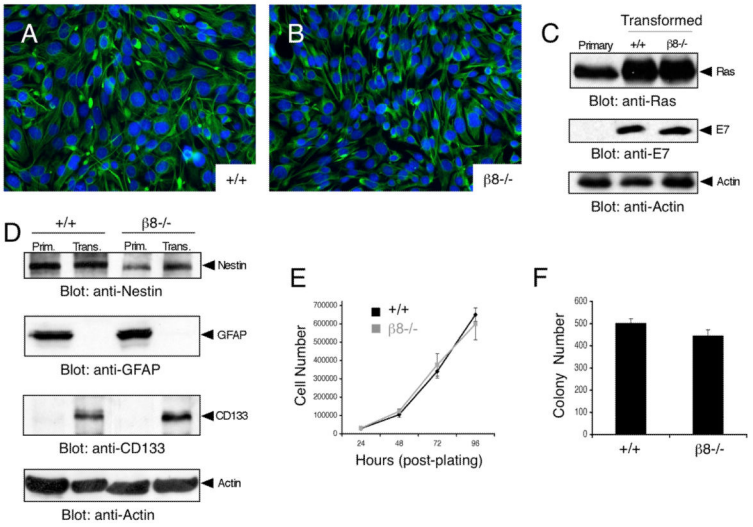

Figure 3. Integrin-independent cell growth in transformed astroglial progenitor cells

(A, B); Immunofluorescence staining reveals that Nestin protein expression is maintained in wild type (A) and β8−/− (B) astroglial progenitor cells that have been transformed with E6/E7 and ^{G12V}H-Ras oncogenes. Note the changes in cell morphologies following transformation, as compared to primary cell morphologies shown in Figures 2B and 2D. **(C);** Detergent-soluble lysates from wild type and β8−/− primary and transformed cells were immunoblotted with antibodies directed against Ras and E7 proteins. **(D);** Lysates prepared from primary and transformed astroglial progenitor cells were immunoblotted with anti-Nestin, anti-CD133/Prominin-1, anti-GFAP and anti-Actin antibodies. Note the increase in CD133 expression and decrease in GFAP expression in transformed cells. Lysates used for these immunoblots are the same as those analyzed in Figure 4A, therefore the actin immunoblots are the same. **(E);** Proliferation indices for adherent wild type and β8−/− transformed astroglial progenitors were determined by counting the total numbers of cells every 24 hours over four consecutive days (n=3 samples per genotype per time point). **(F);** Adhesion-independent cell growth in soft agar was quantified by counting crystal violet-stained colonies (n=3 samples per genotype). The differences in colony numbers formed from wild type and β8−/− cells were not statistically significant. All error bars represent standard deviations.

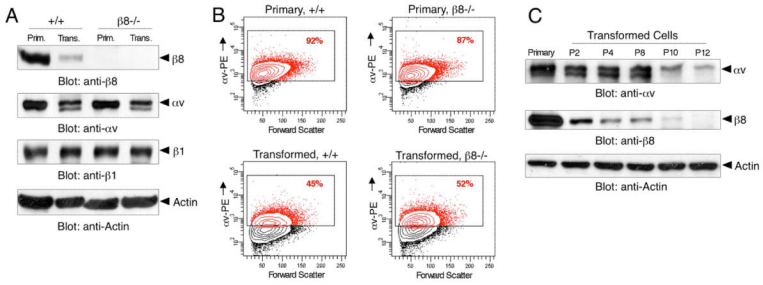

Figure 4. Reduced αvβ8 integrin protein expression following oncogene-mediated astroglial cell transformation

(A); Detergent-soluble lysates from wild type or β8−/− primary (prim.) and transformed (trans.) astroglial progenitors were immunoblotted with antibodies directed against αv, β1, and β8 integrins. In comparison to primary cells, note the progressive reduction in αv and β8 integrin protein expression in transformed cells. The lower molecular weight band in the αv integrin immunoblots (transformed samples) is likely non-glycosylated integrin protein. **(B);** Primary cells (upper panels) and transformed cells (lower panels) were analyzed by fluorescent activated cell sorting using an anti-αv integrin antibody conjugated to phycoerythrein (αv-PE). Percentages of primary and transformed cells expressing cell surface αv integrin protein are indicated in red font. **(C);** Wild type transformed astroglial progenitor cells were propagated over 12 passages. Detergent-soluble lysates (P2 to P12) were then immunoblotted with anti-αv and anti-β8 antibodies. In comparison to unpassaged primary cells (primary), note the progressive reduction in αvβ8 integrin protein expression as transformed cells are passaged.

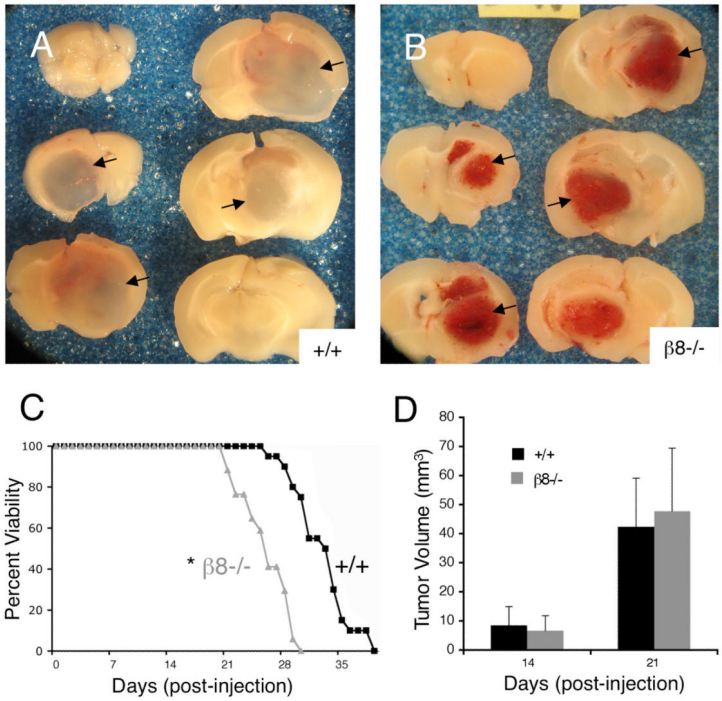

Figure 5. Severe vascular pathologies and diminished survival in mice harboring β8−/− astrocytomas

(A, B); Mice harboring wild type (A) or β8−/− (B) astrocytomas were cardiac-perfused with fixative and then coronally sliced at one millimeter intervals. Shown are representative brain slices from tumor-bearing mice. Note that obvious hemorrhage in β8−/− tumors (arrows, top right panel). **(C);** Kaplan-Meier survival plot for mice harboring wild type (n=20) or β8−/− (n=16) astrocytomas, *p<0.001 at 50% survival. **(D);** A separate cohort of mice harboring wild type and β8−/− astrocytomas were sacrificed at 14 days (n=9 per genotype) and 21 days (n=8 per genotype) after injection. Tumor volumes were quantified in H&E-stained coronal sections by measuring tumor diameters at the largest cross-sectional area; p=0.529 at 14 days (β8−/− samples in comparison to wild type samples); p=0.643 at 21 days (β8−/− samples in comparison to wild type samples). Error bars represent standard deviations.

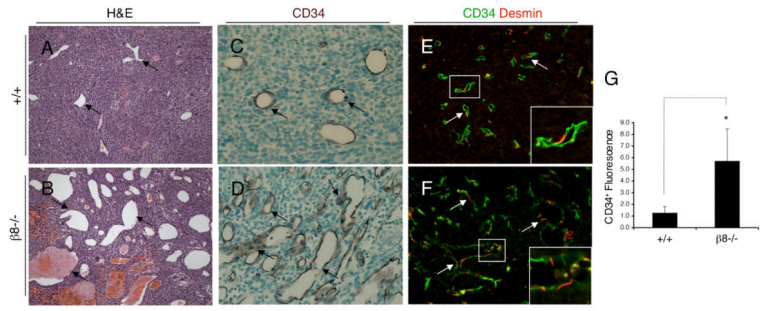

Figure 6. Histological analyses of blood vessels in wild type and β8−/− astrocytomas

(A, B); Coronal sections from wild type (A) or β8−/− (B) astrocytomas stained with hematoxylin and eosin (H&E) and analyzed microscopically (200X). Note the abnormally dilated intratumoral blood vessels in β8−/− astrocytomas (arrows). **(C, D);** Coronal sections from wild type (C) and β8−/− (D) astrocytomas were immunostained with an anti-CD34 antibody and visualized (400X) to label vascular endothelial cells (arrows). **(E, F);** Coronal sections from wild type (E) and β8−/− (F) astrocytomas were immunofluorescently labeled with anti-CD34 to reveal vascular endothelial cells (green) and anti-desmin to reveal vascular pericytes (red). Note that desmin-expressing pericytes are associated with blood vessels within wild type and β8−/− astrocytomas. The boxed areas are shown in higher magnification in the lower right corners of each panel. Magnification for panels E and F, 200X. **(G);** Quantitation of CD34 expression in astrocytoma sections. Sections were immunofluorescently labeled with anti-CD34, and four randomly selected fields were analyzed from wild type and β8−/− tumors (n=5 mice per tumor genotype). In comparison to wild type tumors there is significantly more CD34 immunofluorescence in β8−/− astrocytomas, *p<0.001 for β8−/− samples compared to wild type controls. Error bars represent standard deviations.

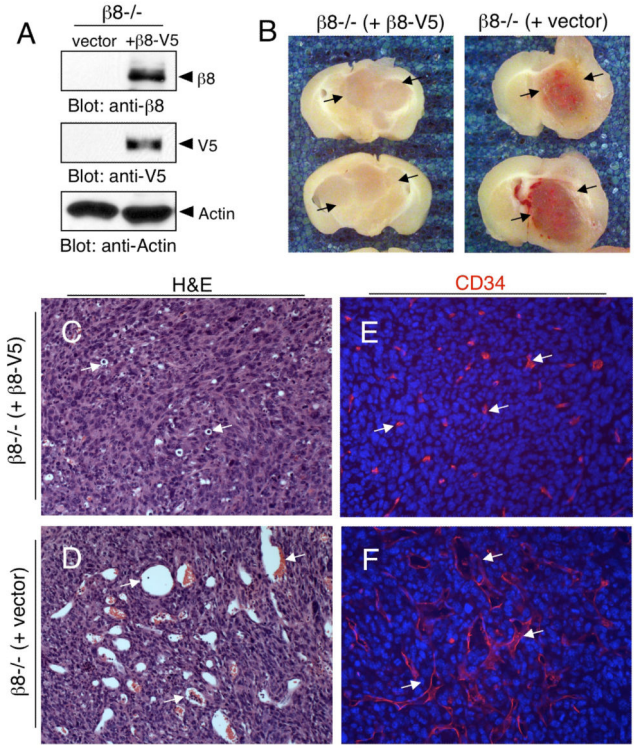

Figure 7. Exogenous expression of β8 integrin rescues astrocytoma-induced vascular pathologies

(A): β8−/− transformed astrocytes were stably transfected with empty vector or a vector expressing human β8 integrin protein tagged at the C-terminus with a V5 epitope (β8-V5). Cell lysates were then immunoblotted with an antibodies directed against β8 integrin (top panel), V5 (middle panel) or actin (bottom panel). **(B);** Mice injected with β8−/− transformed astrocytes stably transfected with empty vector (right panel) or β8−/− cells stably expressing β8-V5 protein (left panel) were cardiac-perfused with fixative and brains were coronally sliced at one millimeter intervals. Note the hemorrhage in β8−/− (empty vector) tumors that is absent in the tumors expressing β8-V5 protein (arrows). **(C, D);** Coronal sections from β8−/− (+ β8V5) astrocytomas (C) or β8−/− (+ vector) astrocytomas (D) were stained with hematoxylin and eosin (H&E). Note that the dilated intratumoral blood vessels in β8−/− tumors are diminished in tumors expressing β8-V5 integrin protein (arrows). **(E, F);** Coronal sections from astrocytomas were immunofluorescently labeled with anti-CD34 to reveal vascular endothelial cells. Note the obvious differences in blood vessel characteristics in the β8−/− +β8-V5 tumors (E) versus β8−/− tumors (F). Sections in panels C-E were analyzed at 200X magnification.

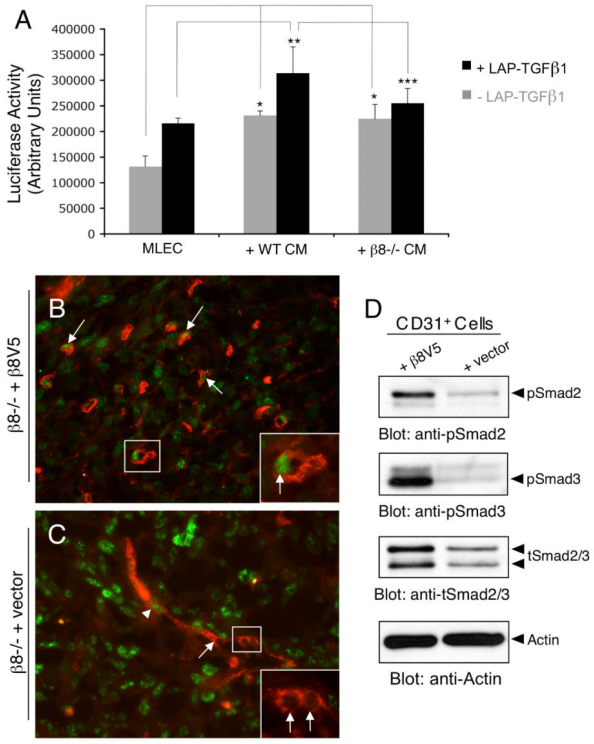

Figure 8. Analysis of β8 integrin-mediated TGFβ activation and signaling

(A); Diminished TGFβ activation in β8−/− cells using a PAI1-lucferase reporter assay. Conditioned media (+/− exogenous LAP-TGFβ1) from wild type (n=3) or β8−/− (n=3) transformed astroglial progenitors was transferred to MLECs stably transfected with PAI1-Luciferase followed by analysis of luciferase activity. Conditioned media from wild type cells pre-treated with LAP-TGFβ1 induced robust luciferase activity; however, note the reduced luciferase activity using conditioned media from β8−/− cells, *p<0.0001 compared to conditioned media without LAP-TGFβ1; **p<0.004 compared to wild type cells; ***p= 0.04 compared to wild type cells. Error bars represent standard deviations. **(B, C);** Fluorescent images (400X) of coronal sections from β8−/− astrocytomas stably expressing β8-V5 integrin protein (B) or β8−/− astrocytomas transfected with empty vector (C). Sections were immunofluorescently labeled with anti-CD31 (red) to visualize vascular endothelial cells and anti-pSmad3 (green) to monitor canonical TGFβ signaling. Note that most vessels within β8 integrin-expressing tumors contain nuclear pSmad3 (arrows in B), whereas vessels within β8−/− tumors are largely negative for nuclear pSmad3 (arrows in C) although some nuclear pSmad3 is detected (arrowhead in C). Boxed areas in B and C are shown at higher magnification in lower right corners. **(D);** Mice injected intracranially with β8−/− (+ vector) cells or β8−/− (+ β8V5) cells were sacrificed, tumors were microdissected, and intratumoral endothelial cells were isolated using magnetic beads coated with anti-CD31 antibodies. Cell lysates were then immunoblotted with antibodies recognizing phosphorylated Smad2/3, total Smad2/3, or actin.